

Supporting Information for ‘How Small is Too Small for the Capillarity Theory?’

Alexandre B. Almeida¹, Sergey V. Buldyrev²,
Adriano M. Alencar¹, Nicolas Giovambattista^{3,4}

¹ *Instituto de Física,
Universidade de São Paulo,
05508-090, São Paulo, SP, Brazil*

² *Department of Physics,
Yeshiva University,
500 West 185th Street,
New York, NY 10033 USA*

³ *Department of Physics,
Brooklyn College of the City University of New York,
Brooklyn, NY 11210 USA*

⁴ *Ph.D. Programs in Chemistry and Physics,
The Graduate Center of the City University of New York,
New York, NY 10016 USA*

We provide additional information related to the results included in the main manuscript.

- Figure S1 complements Figure 3 of the main manuscript by including the water capillary bridge (WCB) profiles studied for all values of surface polarity k and wall separations h . In this case, the WCB profile obtained from MD simulations, $r_{MD}(z)$, is calculated using slabs of thickness $\delta_s = 5 \text{ \AA}$ (shifted every $\delta_z = \delta_s/2$). The WCB profile from CT is obtained by fitting $r_{MD}(z)$ using eq 1 of the main manuscript (all points of $r_{MD}(z)$ are included in the fitting procedure).
- In Figures S2–S5, we study how the profiles of the WCB obtained from MD simulations $r_{MD}(z)$, are affected by varying the thickness of the slabs δ_s used to coarse-grain the density of water from the MD simulations.

Figures S2 and S3 show the WCB profiles obtained for two surface polarities, $k = 0.0$ (hydrophobic) and $k = 0.5$ (hydrophilic), and for $\delta_s = 1.250, 2.500, 2.857, 3.125, 3.333, 4.167, 5.000, 8.333 \text{ \AA}$ ($\delta_z = \delta_s/2$). For simplicity, we only include results for wall separation $h = 20, 25, 50 \text{ \AA}$. The circles are the WCB profiles obtained from MD simulations. Compared to Figure 3 of the main manuscript ($\delta_s = 5 \text{ \AA}$), using a small $\delta_s < 5 \text{ \AA}$ can lead to very small radii of the WCB in the 1-2 slabs closest to the walls. This can be seen clearly in the last two rows of Figures S2 and S3 where the circles at height $\approx h/2$ deviates from the rest of the circles at lower heights. This implies that, for small values δ_s , the 1-2 points closest to each wall should be omitted when fitting $r_{MD}(z)$ using the expression from CT, eq 1 of the main manuscript. Indeed, the dashed lines in Figures S2 and S3 correspond to the fitting profiles of the WCB (from eq 1 of main manuscript) considering all data points of $r_{MD}(z)$. At $\delta_s = 1.250 \text{ \AA}$, the dashed lines clearly deviate from the $r_{MD}(z)$ (circles).

The solid lines in Figure S2 are the profiles of the WCB predicted by CT (eq 1 of main manuscript) when the *one* point closest to the upper and lower walls are removed. Similarly, the solid lines in Figure S3 correspond to the WCB profiles predicted by CT when the *two* points of $r_{MD}(z)$ closest to the upper and lower walls are removed during the fitting procedure.

From the theoretical profiles obtained for the values of δ_s considered, $1.250 \leq \delta_s \leq 12.5 \text{ \AA}$ we extract the water contact angles θ , WCB average curvature H , and the

corresponding error ϵ of the theoretical profile relative to the profile extracted from MD simulations (e.g, solid lines and circles in Figures S2 and S3, respectively). The values of θ , H , and ϵ for the case when *one* point of $r_{MD}(z)$ closest to the upper and lower walls are removed (Figure S2) are shown in Figure S4. The values of θ , H , and ϵ for the case when *two* points of $r_{MD}(z)$ closest to the upper and lower walls are removed (Figure S3) are shown in Figure S5. It follows from Figures S4 and S5 that decreasing δ_s increases both θ and H . This is problematic since θ and H are properties of the WCB that should not vary with the specific procedure employed, as defined by the specific value of δ_s employed. In addition, ϵ also increases with decreasing δ_s . In order to obtain δ_s -independent values of θ and H , while keeping a small error $\epsilon \approx \mathcal{O}(0.1 \text{ \AA})$, one can safely choose $\delta_s > 2 - 3 \text{ \AA}$; see Figures S4 and S5.

- Figure S6 complements Figure 5 of the main manuscript by including the WCB profiles studied for all values of surface polarity k and wall separations h . In this case, the WCB profile obtained from the MD simulations, $r_{MD}(z)$, is calculated using slabs of thickness $\delta_s = 2.5 \text{ \AA}$ ($\delta_z = \delta_s/2$). The WCB profile from CT is obtained by fitting $r_{MD}(z)$ using eq 1 of the main manuscript and omitting the *two* points of $r_{MD}(z)$ closest to the upper and lower walls during the fitting procedure.
- Figure S7 shows profiles of the WCB obtained from MD simulations (circles) using slabs of thickness $\delta_s = 2.5 \text{ \AA}$ ($\delta_z = \delta_s/2$). The solid lines are the profiles of the WCB obtained from eq 1 of the main manuscript when the *one* point of $r_{MD}(z)$ closest to the upper and lower walls are removed. The fitting parameters for the theoretical WCB profiles are given in Tables S1 and S2.

The water contact angles obtained from the WCB included in Figure S7 are shown in Figure S8 (see also Table S3).

- Figure S9 complements Figure 10 of the main manuscripts. It includes the density profile of water within the capillary bridge along the z-axis (perpendicular to the walls) for all values of h and surface polarities k studied.
- Next, we provide a brief proof for the modified Young's equation, eq 3 of the main manuscript, for the case of axis-symmetric capillary bridges:

$$\cos \theta = \cos \theta_\infty - (\tau/\gamma) 1/r_b. \quad (1)$$

We use this equation to calculate the solid-liquid-vapor line tension τ . In this expression, γ is the liquid-vapor surface tension, θ is the water contact angle of the capillary bridge at a given wall separation h , and θ_∞ is the ‘macroscopic’ contact angle; $r_b = r(\pm h/2)$ is the radius of the capillary bridge base.

The free energy of the capillary bridge, including the contribution of τ , is given by

$$\mathcal{F} = \Omega\mathcal{F}_{\text{bulk}} + 2\gamma_{\text{LS}}A_{\text{LS}} + 2\gamma_{\text{SG}}(A_{\text{T}} - A_{\text{LS}}) + \gamma_{\text{LG}}A_{\text{LG}} + \tau L + c \quad (2)$$

where Ω is the volume of the capillary bridge and $\mathcal{F}_{\text{bulk}}$ is the bulk liquid free energy; we assume Ω and $\mathcal{F}_{\text{bulk}}$ are constants (independent of h). γ_{LG} , γ_{LS} and γ_{SG} are, respectively, the liquid-gas, liquid-solid, and solid-gas surface (for simplicity we will denote $\gamma_{\text{LG}} = \gamma$). A_{LG} , A_{LS} , A_{SG} are the corresponding surface areas of the capillary bridge and A_{T} is the surface area of the wall. L is the total length of the contact lines formed at the intersections of the liquid-gas, liquid-solid, and solid-gas interfaces. c is an arbitrary constant which is chosen to be $c = -2\gamma_{\text{SG}}A_{\text{T}} - \Omega\mathcal{F}_{\text{bulk}}$.

It follows from Figure 1 of the main manuscript that

$$A_{\text{LS}} = \pi [r^2(-h/2) + r^2(h/2)], \quad (3)$$

and

$$L = 2\pi [r(-h/2) + r(h/2)], \quad (4)$$

where $r(z)$ is the profile of the capillary bridge. The area of an axis-symmetric capillary bridge is given by²

$$A_{\text{LG}} = 2\pi \int_{-h/2}^{h/2} r\sqrt{1 + r'(z)^2} dz. \quad (5)$$

The contact angle of the macroscopic capillary bridge must obey Young’s equation, i.e,

$$\cos \theta_\infty = (\gamma_{\text{SG}} - \gamma_{\text{SL}})/\gamma. \quad (6)$$

Hence, by combining eqs 3, 4, 5, and 6 into eq 2 one obtains the following expression for the free energy of the capillary bridge,

$$\begin{aligned} \frac{\mathcal{F}}{2\gamma\pi} = & \int_{-h/2}^{h/2} r\sqrt{1 + r'^2} dz - \cos \theta_\infty [r^2(-h/2) + r^2(h/2)] + \\ & + (\tau/\gamma) [r(-h/2) + r(h/2)]. \end{aligned} \quad (7)$$

Now, in equilibrium, the free energy must be a minimum. In the context of variational calculus, this implies that $\delta\mathcal{F} = 0$ under small variations of the equilibrium profile of the capillary bridge, $r(z) \rightarrow r(z) + \delta(z)$ where $\delta(z)$ is an arbitrary small function of z .

Since we are considering that the capillary bridge volume

$$\Omega = \pi \int_{-h/2}^{h/2} r^2 dz \quad (8)$$

is constant, minimizing \mathcal{F} is equivalent to minimizing the functional $\mathcal{L} = \mathcal{F} - 2\gamma H\Omega$, where $2\gamma H$ is a Lagrange multiplier. It follows from eqs 7 and 8 that

$$\begin{aligned} \frac{\mathcal{L}}{2\gamma\pi} = & \int_{-h/2}^{h/2} (r\sqrt{1+r'^2} - Hr^2) dz - \cos\theta_\infty [r^2(-h/2) + r^2(h/2)] + \\ & +(2\tau/\gamma) [r(-h/2) + r(h/2)]. \end{aligned} \quad (9)$$

The variation of \mathcal{L} is given by

$$\begin{aligned} \frac{\delta\mathcal{L}}{2\pi\gamma} = & \int_{-h/2}^{h/2} (\delta\sqrt{1+r'^2} - 2Hr\delta) dz + \\ & + \int_{-h/2}^{+h/2} r \frac{r'\delta'}{\sqrt{1+r'^2}} dz + \\ & + \frac{2\tau}{\gamma} [\delta(-h/2) + \delta(h/2)] - \\ & - \cos\theta_\infty [r(-h/2)\delta(-h/2) + r(h/2)\delta(h/2)]. \end{aligned} \quad (10)$$

Integrating by parts the expression $\int_{-h/2}^{+h/2} r \frac{r'\delta'}{\sqrt{1+r'^2}} dz$, we have:

$$\begin{aligned} \frac{\delta\mathcal{L}}{2\pi\gamma} = & \int_{-h/2}^{+h/2} (\delta\sqrt{1+r'^2} - 2Hr\delta) dz + \\ & + r \frac{r'\delta}{\sqrt{1+r'^2}} \Big|_{-h/2}^{+h/2} - \\ & - \int_{-h/2}^{h/2} \frac{d}{dz} \left[\frac{rr'}{\sqrt{1+r'^2}} \right] \delta dz + \\ & + \frac{2\tau}{\gamma} \pi [\delta(-h/2) + \delta(h/2)] - \\ & - \cos\theta_\infty [r(-h/2)\delta(-h/2) + r(h/2)\delta(h/2)]. \end{aligned} \quad (11)$$

Since $\delta\mathcal{L} = 0$, both the integral and the non-integral parts of eq 11 must equal zero for any arbitrary function $\delta(z)$. The integral part gives the Euler's equation that can

be solved to obtain the theoretical capillary bridge profile $r(z)$. The non-integral part of eq 11 must satisfy

$$\begin{aligned} & \delta(h/2)r(h/2) \left[\frac{r'(h/2)}{\sqrt{1+r'(h/2)^2}} - \cos\theta_\infty + \frac{\tau}{\gamma r(h/2)} \right] + \\ & + \delta(-h/2)r(-h/2) \left[-\frac{r'(-h/2)}{\sqrt{1+r'(-h/2)^2}} - \cos\theta_\infty + \frac{\tau}{\gamma r(h/2)} \right] = 0 \quad (12) \end{aligned}$$

for arbitrary values of $\delta(h/2)$ and $\delta(-h/2)$. This implies that the coefficients in front of $\delta(h/2)$ and $\delta(-h/2)$ in eq 12 are equal to zero. Note that geometrically $\pm r'(\pm h/2)/\sqrt{1+r'(\pm h/2)^2} = \cos\theta$, where θ is the contact angle on both sides of the bridge. Hence the minimization condition gives $\cos\theta = \cos\theta_\infty - (\tau/\gamma) 1/r(\pm h/2)$ which is the modified Young's equation.

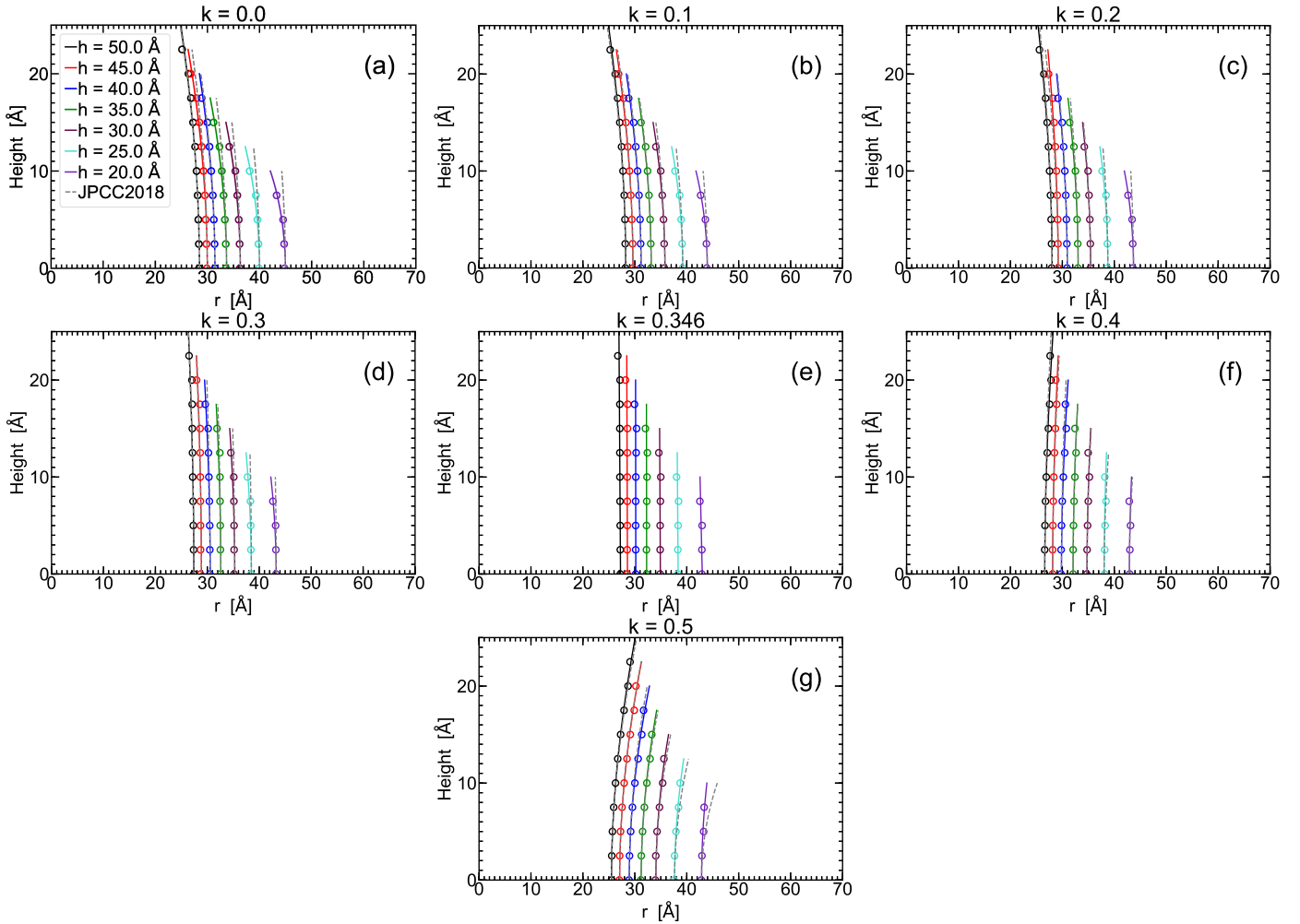


Figure S1: Same as Figure 3 of the main manuscript but including the average profile of the water capillary bridges obtained for all surface polarities k and wall separations h studied. Circles represent the capillary bridge profiles obtained from MD simulations using slabs of thickness $\delta_s = 5.0 \text{ \AA}$ and located every $\delta_z = \delta_s/2 = 2.5 \text{ \AA}$. The solid lines are the theoretical profiles based on eq 1 of the main manuscript that fit the MD data; the corresponding fitting parameters are given in Tables 1–2 of the main manuscript. The dashed gray lines are the theoretical profiles obtained when the contact angles in Tables 1–2 of the main manuscript are substituted by the contact angles that we reported in ref ¹ obtained for $h > 50 \text{ \AA}$. Dashed-lines in, e.g, (a)-(d), and (g), deviates from the MD simulations data indicating that the contact angles calculated at $h = 50 \text{ \AA}$ do not necessarily apply as $h \rightarrow 20 \text{ \AA}$.

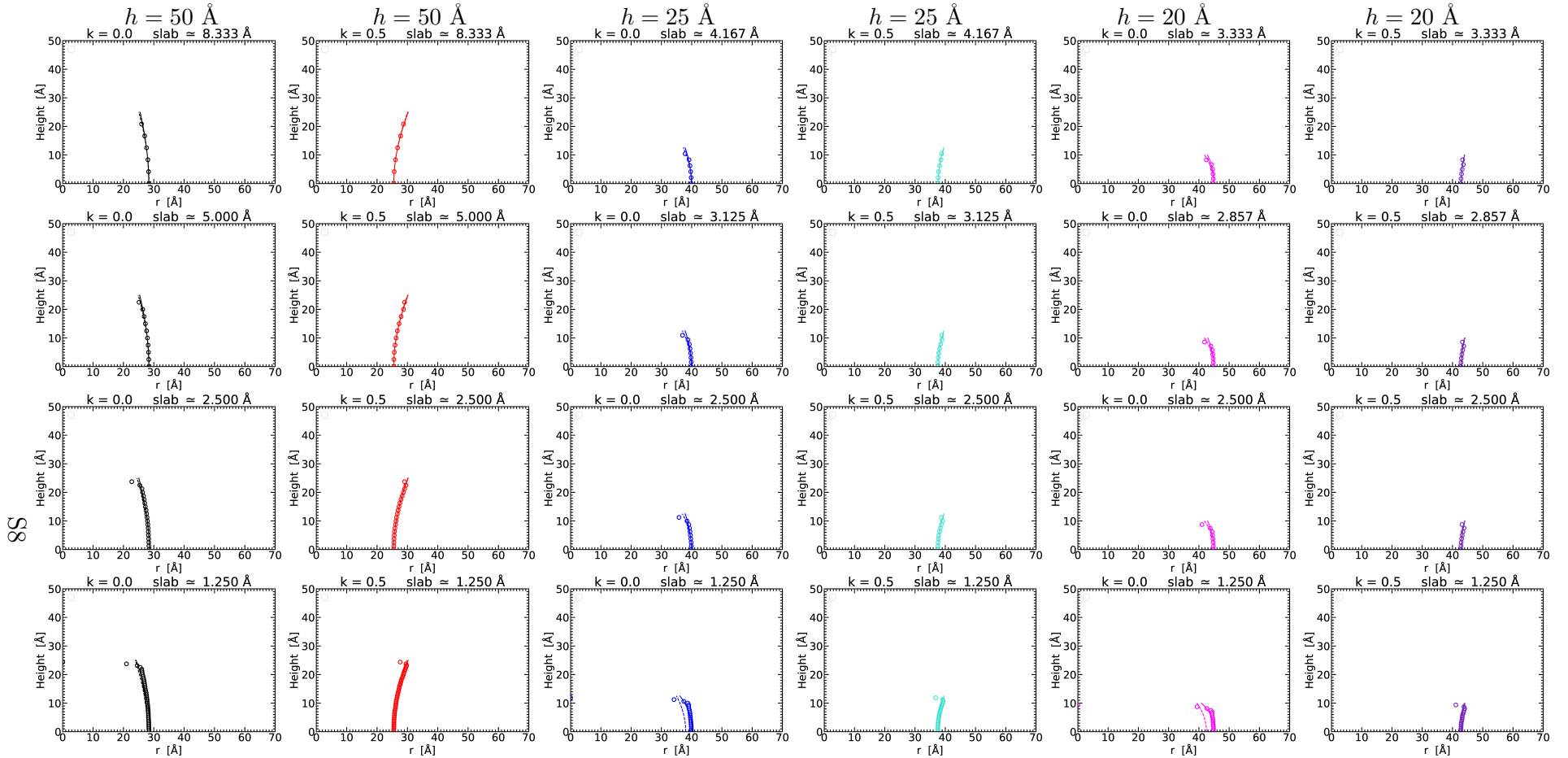


Figure S2: Examples of water capillary bridge profiles obtained from MD simulations using slabs of thickness $1.25 \leq \delta_s \leq 8.33 \text{ \AA}$ ($\delta_z = \delta_s/2$) and for $h = 20, 25, 50 \text{ \AA}$. Only capillary bridges formed between walls of surface polarities $k = 0.0$ (hydrophobic) and $k = 0.5$ (hydrophilic) are included. Circles represent the capillary bridge profiles obtained from MD simulations ($r_{MD}(z)$); solid lines are the theoretical profiles based on eq 1 of the main manuscript that fit $r_{MD}(z)$. The *one* point of $r_{MD}(z)$ (circles) closest to the upper and lower walls are omitted during the fitting procedure. Dashed lines correspond to the theoretical profiles of the WCB obtained by considering all data points of $r_{MD}(z)$.

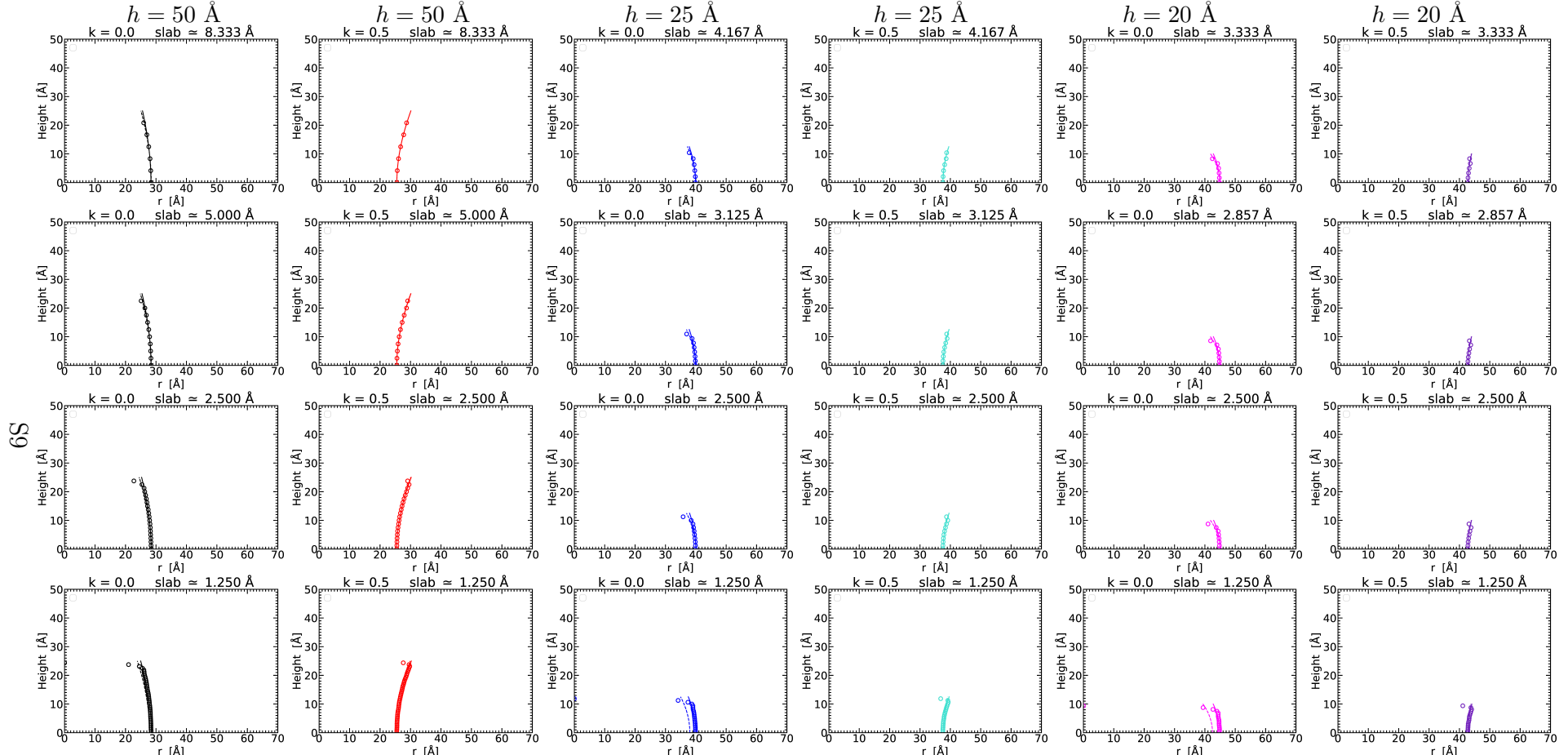


Figure S3: Same as Figure S2 but removing the *two* points of $r_{MD}(z)$ (circles) closest to the upper and lower walls during the fitting procedure followed to obtain the theoretical profile of the WCB (solid lines).

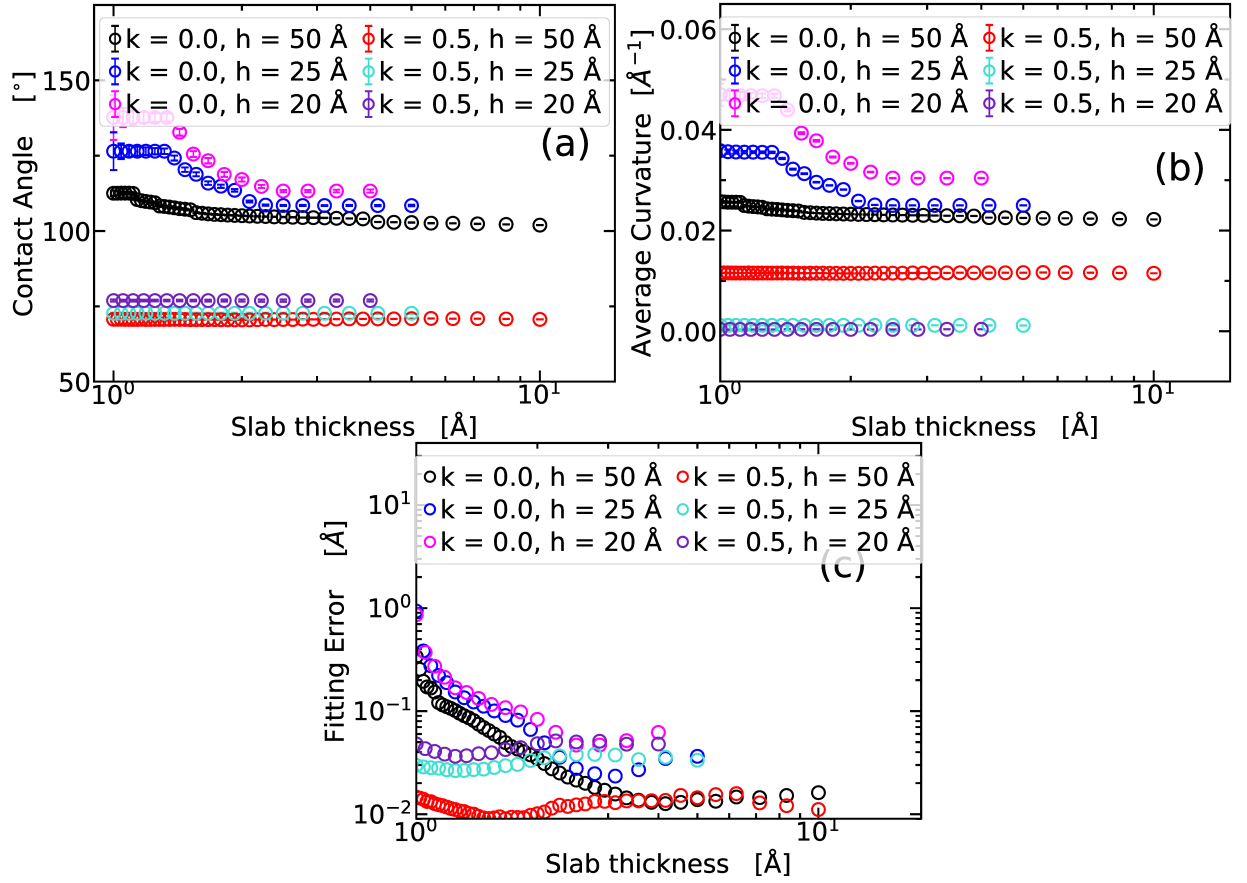


Figure S4: (a) Water contact angle θ and (b) average curvature H of the water capillary bridges formed between walls of different surface polarities k separated by distance h . The capillary bridge profiles, from which θ and H are obtained, are calculated from the MD simulations using slabs of thickness δ_s ($\delta_z = \delta_s/2$). The corresponding theoretical profile is obtained by removing the *one* point of $r_{MD}(z)$ closest to the upper and lower walls during the fitting procedure; examples of the MD and theoretical bridge profiles are shown in Figure S2. Both quantities θ and H are, in general, sensitive to δ_s but become δ_s -independent for $\delta_s > 2 - 3$ Å (i.e., at these conditions, θ and H are independent of the fitting procedure). (c) Error ϵ of the WCB profile obtained during the fitting procedure relative to the corresponding profile obtained from MD simulations (see main manuscript). The minimum value of δ_s for which θ and H are independent of the procedure followed, and for which the capillary profile has a small error, $\epsilon = \mathcal{O}(0.1)$ Å, is approximately $\delta_s > 2 - 3$ Å.

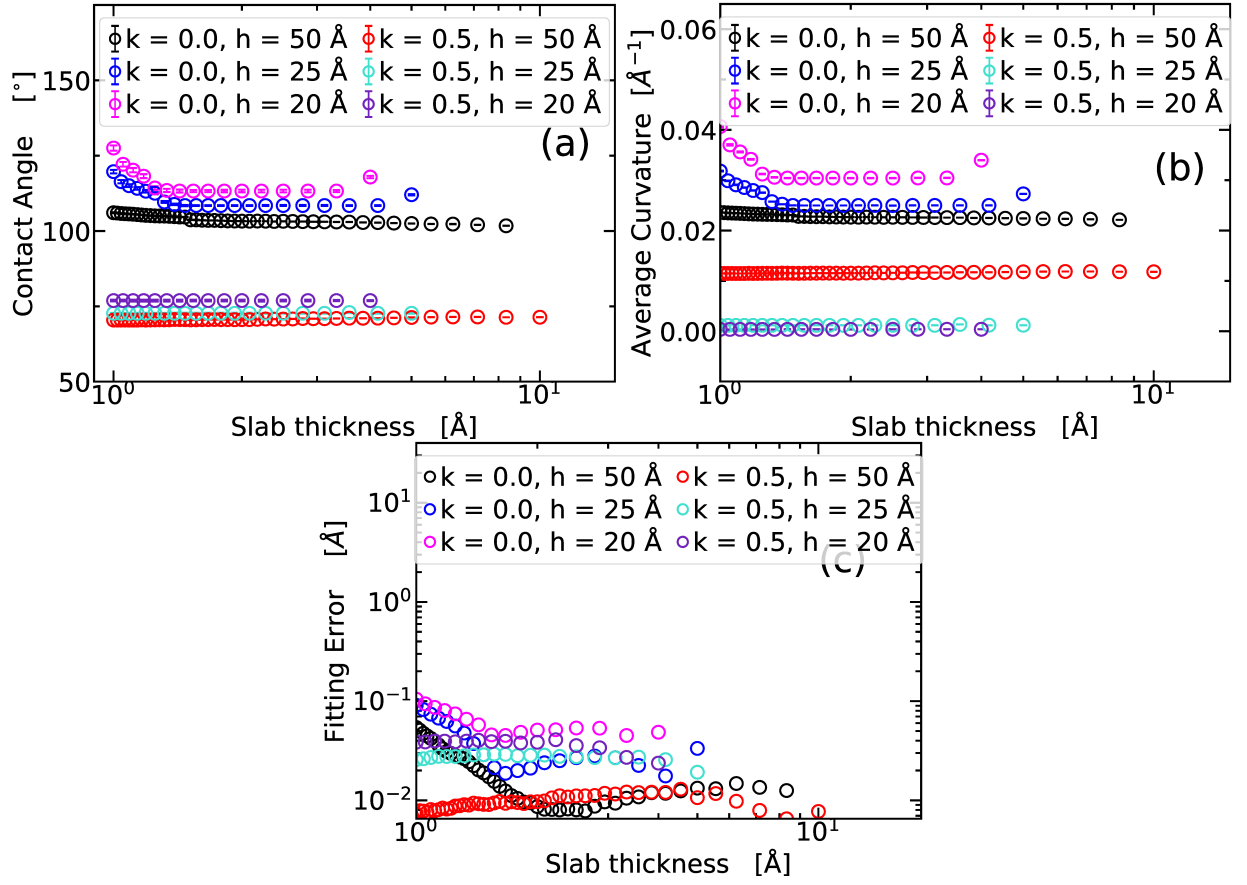


Figure S5: Same as Figure S4 but removing *two* points of $r_{MD}(z)$ closest to the upper and lower walls during the fitting procedure followed to calculate the theoretical capillary profiles. Examples of the MD and theoretical capillary bridge profiles are shown in Figure S3. The minimum value of δ_s for which θ and H are independent of the procedure followed, and for which the capillary profile has a small error, $\epsilon = \mathcal{O}(0.1 \text{ \AA})$ is approximately $\delta_s > 1 - 2 \text{ \AA}$.

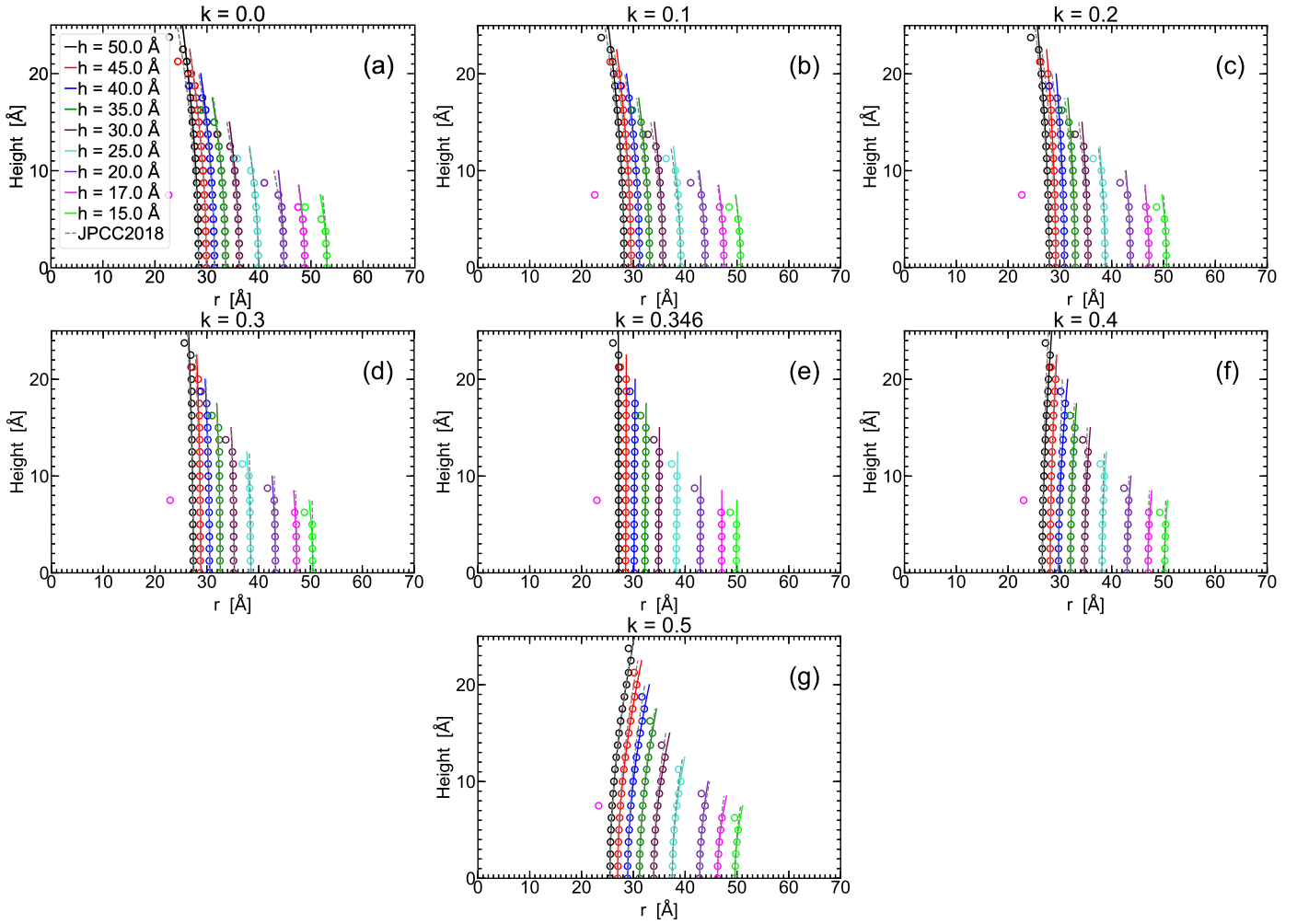


Figure S6: Same as Figure 5 of the main manuscript but including the average profiles of water capillary bridges for all surface polarities k and wall separations h studied. The average water capillary bridges obtained from MD simulations ($r_{MD}(z)$, circles) are calculated using slabs of thickness $\delta_s = 2.5 \text{ \AA}$ (located every $\delta_z = \delta_s/2$). The solid lines are the theoretical profiles based on eq 1 of the main manuscript that fit the MD data; the corresponding fitting parameters are given in Tables 4 and 5 of the main manuscript. The dashed gray lines are the theoretical profiles obtained when the contact angles in Tables 4 and 5 of the main manuscript are substituted by the contact angles that we reported in ref¹, obtained for $h \geq 50 \text{ \AA}$. Due to the small value of δ_s , the *two* data points (circles) closest to the upper ($z = h - \delta_z, h - 2\delta_z$) and lower ($z = -(h - \delta_z), -(h - 2\delta_z)$) walls are excluded in the calculation of the theoretical profiles (solid and dashed lines).

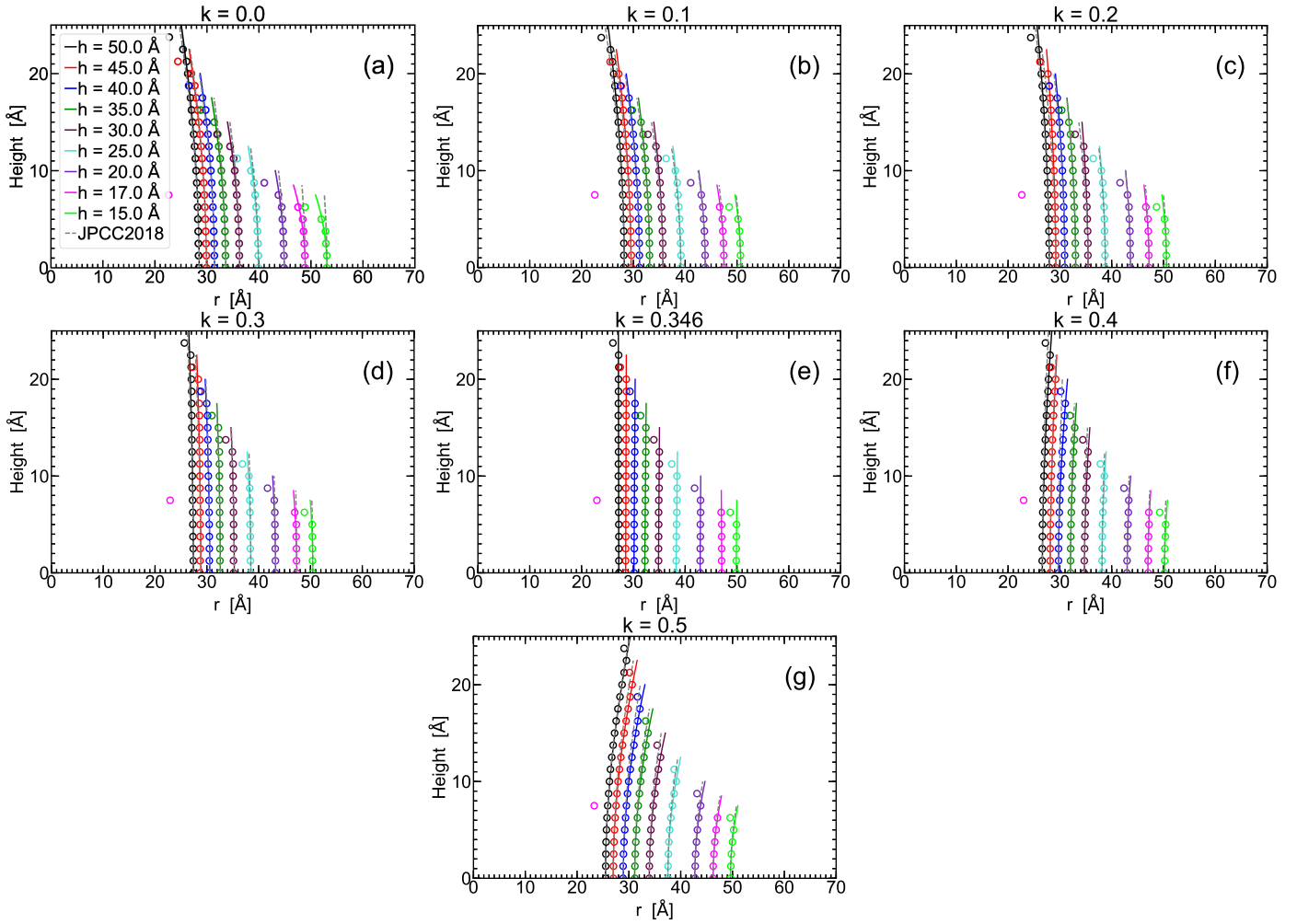


Figure S7: Same as Figure 3 of the main manuscript but with the water capillary bridges from MD simulations ($r_{MD}(z)$, circles) calculated using slabs of thickness $\delta_s = 2.5 \text{ \AA}$ (located every $\delta_z = \delta_s/2 \text{ \AA}$). The solid lines are the theoretical profiles based on eq 1 of the main manuscript that fit $r_{MD}(z)$. The data point of $r_{MD}(z)$ (circles) closest to the upper ($z = h - \delta_z$) and lower ($z = -(h - \delta_z)$) walls are excluded in the calculation of the theoretical profiles (solid lines). The corresponding fitting parameters are given in Tables S1 and S2. The dashed gray lines are the theoretical profiles obtained when the contact angles in Tables S1 and S2 are substituted for the contact angles that we reported in ref¹, obtained for $h \geq 50 \text{ \AA}$.

TABLE S1: Parameters obtained by fitting the capillary profiles obtained from the MD simulations ($r_{MD}(z)$, circles in Figure S7) using eq 1 of the main manuscript for walls with surface polarity $k = 0.0, 0.1, 0.2, 0.3$ (see also Table S2). The corresponding theoretical profiles are indicated by the solid lines in Figure S7. R_1 ($r_0 = R_1$) and R_2 are the radii of curvature of the water capillary bridge's neck. $H = \frac{1}{2}(\frac{1}{R_1} + \frac{1}{R_2})$ is the average surface curvature of the capillary bridge, θ is the corresponding contact angle, and ϵ is the error of the theoretical profile relative to $r_{MD}(z)$. Errors in r_0 , and R_2 are ± 0.05 Å.

$k = 0.0$						$k = 0.1$				
h	r_0 (Å)	R_2 (Å)	H (Å $^{-1}$)	θ (°)	ϵ (Å)	r_0 (Å)	R_2 (Å)	H (Å $^{-1}$)	θ (°)	ϵ (Å)
50.0	28.5	90.2	0.0231	104.6	0.021	28.2	98.2	0.0228	103.4	0.01
45.0	29.9	77.1	0.0232	106.0	0.018	29.6	89.8	0.0225	103.6	0.012
40.0	31.5	74.3	0.0226	105.1	0.018	31.2	79.4	0.0223	104.1	0.008
35.0	33.6	58.9	0.0234	107.1	0.021	33.2	72.7	0.022	103.8	0.01
30.0	36.3	50.4	0.0237	107.4	0.028	35.7	65.8	0.0216	103.2	0.013
25.0	39.9	42.0	0.0244	107.6	0.026	39.2	54.3	0.022	103.5	0.015
20.0	44.9	30.8	0.0274	109.4	0.037	43.9	42.1	0.0233	104.0	0.012
17.0	48.9	17.8	0.0383	119.3	0.057	47.5	28.7	0.0279	107.7	0.031
15.0	53.1	14.3	0.0444	122.6	0.056	50.7	27.0	0.0284	106.6	0.017

$k = 0.2$						$k = 0.3$				
h	r_0 (Å)	R_2 (Å)	H (Å $^{-1}$)	θ (°)	ϵ (Å)	r_0 (Å)	R_2 (Å)	H (Å $^{-1}$)	θ (°)	ϵ (Å)
50.0	27.9	131.5	0.0217	99.8	0.008	27.4	349.9	0.0197	93.6	0.025
45.0	29.2	140.5	0.0207	98.6	0.009	28.8	321.6	0.0189	93.7	0.032
40.0	31.0	110.7	0.0207	100.0	0.012	30.6	230.5	0.0185	94.8	0.019
35.0	33.1	93.3	0.0205	100.6	0.014	32.6	235.7	0.0175	94.2	0.028
30.0	35.4	99.5	0.0191	98.7	0.008	35.3	186.1	0.0169	94.6	0.029
25.0	38.8	72.4	0.0198	100.1	0.016	38.5	116.2	0.0173	96.3	0.024
20.0	43.6	55.2	0.0205	100.7	0.016	43.3	93.4	0.0169	96.3	0.02
17.0	47.2	39.2	0.0233	102.8	0.028	47.4	61.1	0.0187	98.2	0.028
15.0	50.6	33.1	0.025	103.5	0.019	50.5	62.1	0.018	97.2	0.028

TABLE S2: Same as Table S1 for the theoretical profiles of Figure S7 corresponding to surface polarities $k = 0.346$, 0.4 and 0.5.

$k = 0.346$						$k = 0.4$				
h	r_0 (Å)	R_2 (Å)	H (Å $^{-1}$)	θ (°)	ϵ (Å)	r_0 (Å)	R_2 (Å)	H (Å $^{-1}$)	θ (°)	ϵ (Å)
50.0	27.2	∞	0.0184	90.2	0.007	26.6	-163.2	0.0157	82.5	0.008
45.0	28.5	∞	0.0175	89.7	0.004	28.1	-195.8	0.0152	84.1	0.011
40.0	30.1	∞	0.0166	89.3	0.01	29.7	-113.8	0.0124	80.7	0.006
35.0	32.2	∞	0.0155	89.1	0.008	32.1	-137.4	0.012	83.0	0.006
30.0	34.8	∞	0.0144	89.2	0.008	34.7	-111.0	0.0099	82.4	0.008
25.0	38.2	∞	0.0131	88.8	0.007	38.1	-102.2	0.0082	83.0	0.01
20.0	42.9	∞	0.0117	89.3	0.004	43.0	-77.4	0.0052	82.5	0.017
17.0	47.1	∞	0.0106	90.6	0.015	47.0	-71.3	0.0036	83.0	0.024
15.0	49.8	∞	0.01	89.0	0.002	50.2	-50.8	0.0001	81.3	0.011

$k = 0.5$					
h	r_0 (Å)	R_2 (Å)	H (Å $^{-1}$)	θ (°)	ϵ (Å)
50.0	25.5	-61.7	0.0115	70.6	0.012
45.0	27.0	-53.3	0.0092	68.8	0.006
40.0	28.9	-47.9	0.0069	68.0	0.007
35.0	31.1	-44.4	0.0048	68.5	0.01
30.0	33.9	-37.6	0.0014	67.6	0.007
25.0	37.5	-33.1	-0.0018	68.4	0.011
20.0	42.7	-26.8	-0.007	68.3	0.013
17.0	46.2	-23.7	-0.0103	69.0	0.009
15.0	49.6	-20.7	-0.0141	68.6	0.011

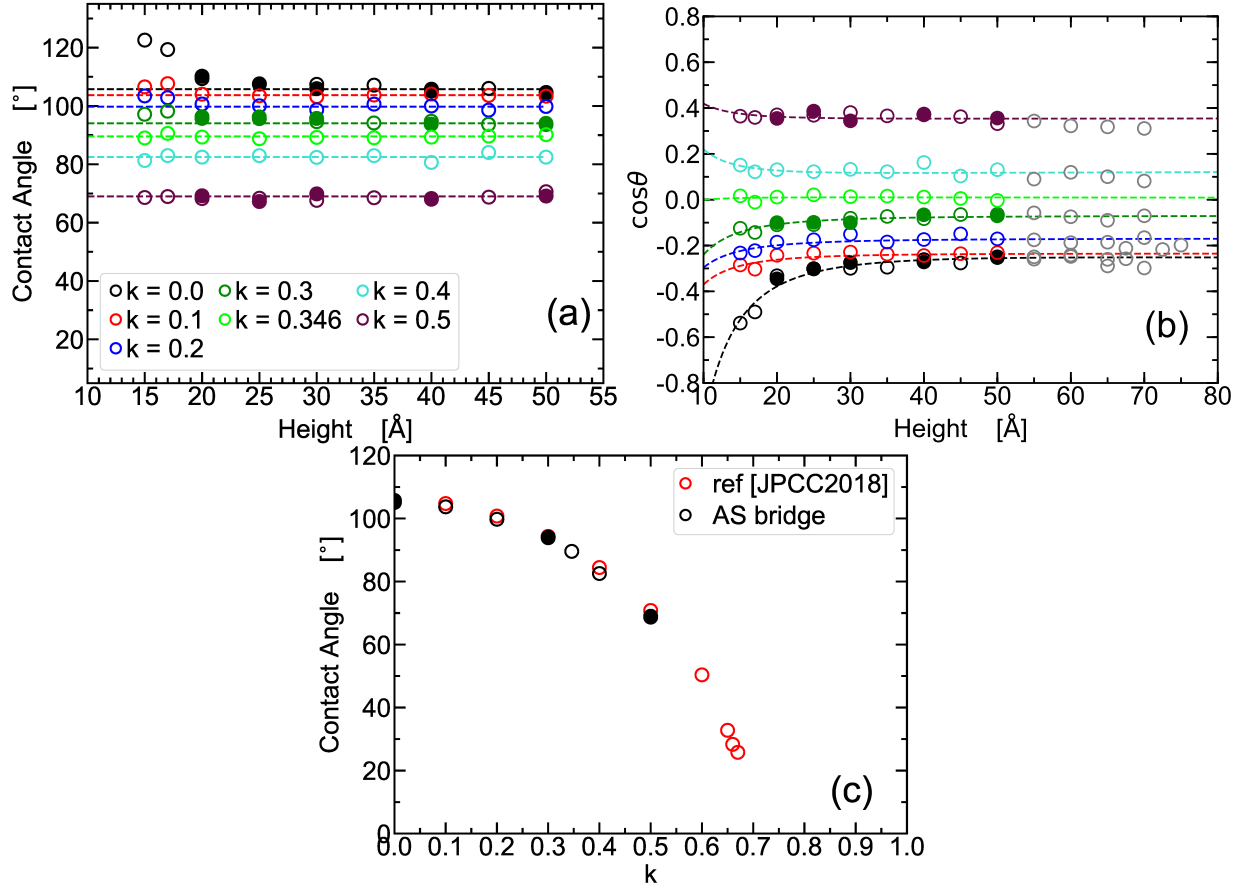


Figure S8: (a) Water contact angle $\theta(h)$ obtained from the theoretical profiles of the WCB corresponding to the solid lines in Figure S7 (see also Tables S1 and S2). The dashed lines indicates the contact angle averaged over $h > 50$ Å. (b) Cosine of the contact angles shown in (a). The gray circles are the values of $\cos\theta(h)$ obtained in ref¹ for $h \geq 50$ Å. The dashed lines are the best fit using the equation $\cos\theta(h) = a/h^2 + b/h + \cos\theta_\infty$; parameters a , b , and $\cos\theta_\infty$ are given in Table S3. (c) Average contact angle obtained from (a) (for $30 < h \leq 50$ Å; black circles) as a function of the surface polarity k . For comparison, we include the average contact angles from ref¹ (for $h \geq 50$ Å; red circles). Error bars are smaller than the symbol sizes. Empty and solid circles are used to distinguished among independent simulations at same k and h .

TABLE S3: Fitting parameters for $\cos \theta$ in Figure S8b using the expression $\cos \theta(h) = a/h^2 + b/h + \cos \theta_\infty$. Units of a and b are Å; $\cos \theta_\infty$ has no units.

k	a	b	$\cos \theta_\infty$
0.0	-98.2037	2.7682	-0.2712
0.1	-16.6621	0.3359	-0.2370
0.2	-13.6080	0.0944	-0.1696
0.3	-19.0635	0.2158	-0.0711
0.346	-2.4490	0.1615	0.0075
0.4	18.9702	-0.9935	0.1298
0.5	10.6159	-0.4551	0.3585

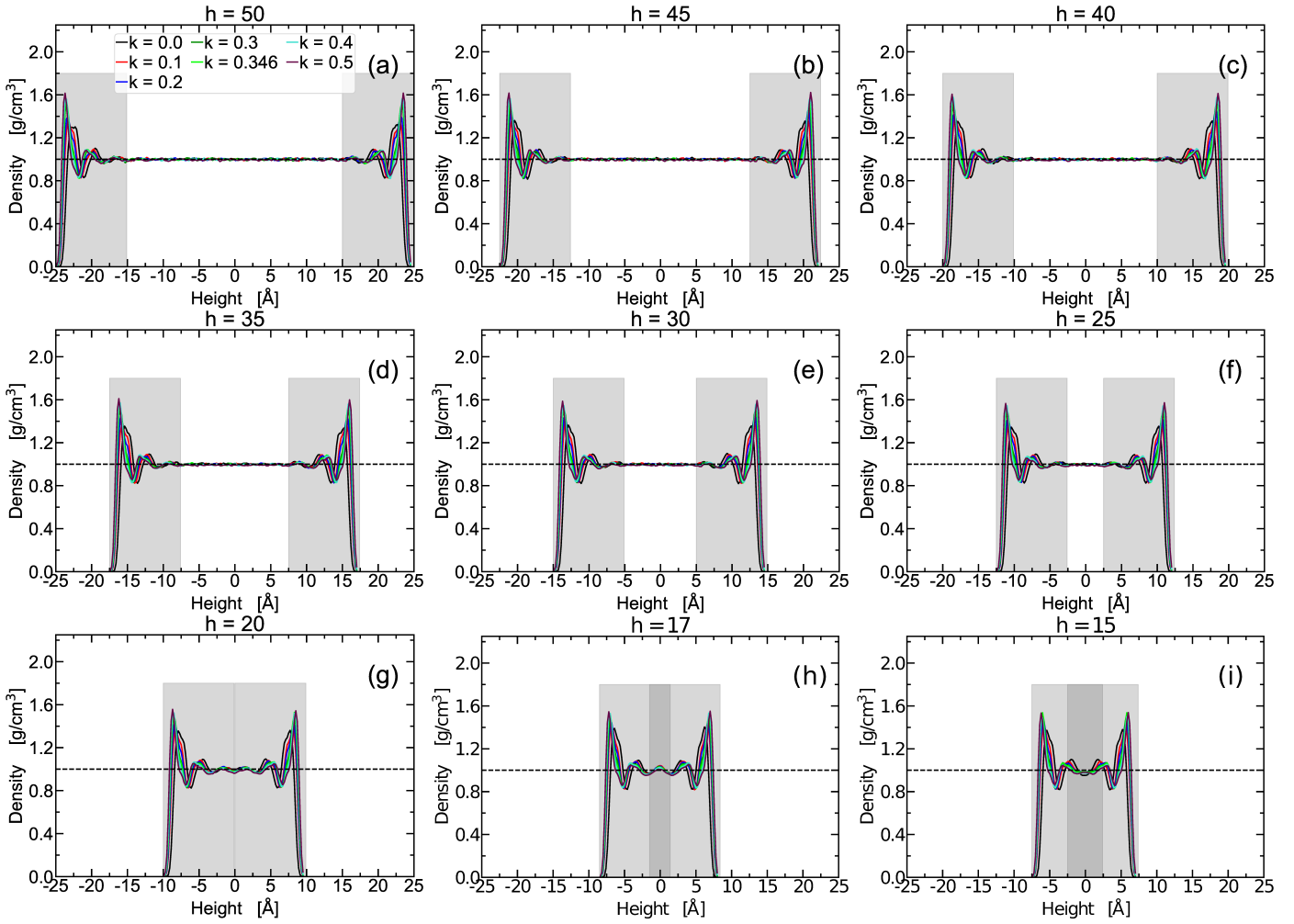


Figure S9: Same as Figure 10 of the main manuscript but including the water density profiles of the water capillary bridges obtained for all surface polarities k and wall separations h studied. The gray regions expanding a distance $\Delta z \approx 10 \text{ \AA}$ mark the regions next to the walls where the density profiles show oscillation, i.e., where water molecules arrange into well-separated layers. Beyond these gray regions, the water density within the capillary bridge matches the density of bulk SPC/E water at $P = 0.1 \text{ MPa}$ and $T = 300 \text{ K}$ (dashed line). CT assumes that the water bridge is composed of solid-liquid and vapor-liquid interfaces enclosing a volume of bulk-like water. However, bulk-like water is not found at $h \leq 20 \text{ \AA}$.

-
- (1) Almeida, A. B.; Giovambattista, N.; Buldyrev, S. V.; Alencar, A. M. Validation of Capillarity Theory at the Nanometer Scale. II: Stability and Rupture of Water Capillary Bridges in Contact with Hydrophobic and Hydrophilic Surfaces. *J. Phys. Chem. C* **2018**, *122*, 1556–1569.
 - (2) de Gennes, P.; Brochard-Wyart, F.; Quéré, D. *Capillarity and Wetting Phenomena: Drops, Bubbles, Pearls, Waves*; Springer: New York, N.Y., 2004.